

# Effect of Al doping on the properties of electrodeposited ZnO nanostructures

Ouidad Baka, Mohamed Redha Khelladi and Amor Azizi

Laboratoire de Chimie, Ingénierie Moléculaires et Nanostructures, Université de Sétif-1, 19000 Sétif, Algeria.

Received: 30 April 2014, accepted 26 May 2014

## Abstract

In this study, Al-doped zinc oxide (AZO) nanostructures are prepared on polycrystalline fluorine-doped tin oxide (FTO)-coated conducting glass substrates from nitrates baths by the electrodeposition process at 70 °C. The electrochemical, morphological, structural and optical properties of the AZO nanostructures were investigated in terms of different Al concentration in the starting solution. It was found from the Mott-Schottky (M-S) plot that the carrier density of AZO nanostructures varied between  $3.11 \times 10^{19}$  to  $5.56 \times 10^{19}$   $\text{cm}^{-3}$  when the Al concentration was between 0 and 5 mM. Atomic force microscopic (AFM) images reveal that the concentration of Al has a very significant influence on the surface morphology and roughness of AZO thin films. X-ray diffraction (XRD) patterns demonstrate preferential (002) crystallographic orientation having c-axis perpendicular to the surface of the substrate and average crystallites size of the films was about 23–36 nm. As compared to pure ZnO, Al-doped ZnO exhibited lower crystallinity and there is a shift in the (002) diffraction peak to higher angles. ZnO nanostructures were found to be highly transparent and had an average transmittance of 80 % in the visible range of the spectrum. After the incorporation of Al content into ZnO the average transmittance increased and the band-gap tuning was also achieved (from 3.22 to 3.47 eV).

Keywords: Al-doped ZnO ; carrier density ; electrodeposition ; nanostructures ; XRD.

## 1. Introduction

Metal oxide semiconductor films have been widely studied in recent years due to their optical and electrical properties. ZnO is both transparent in the visible region and electrically conductive especially when doped with appropriate metals such as Ga or Al [1]. Doped ZnO thin films are of technological importance because of their great potential for various applications such as transparent conducting electrodes (TCOs), insulating or dielectric layers, light-emitting diodes (LEDs) and for solar cells [1, 2], etc. Al-doped ZnO thin films are prepared by different techniques such as sol-gel, spray pyrolysis, pulsed laser deposition (PLD), magnetron sputtering, and metal organic chemical vapor deposition (MOCVD) [8-12]. Amongst all other methods as mentioned above, electrochemical deposition is one of the most attractive methods for the synthesis of nanostructures of semiconductors oxides [3, 4]. It provides advantages such as the ability to use a low synthesis

temperature, low costs, and a high purity in the products. Also, electrodeposition allows the stoichiometry, thickness, and microstructure of the films to be controlled by adjusting the deposition parameters.

In the present paper we have prepared Al-doped ZnO nanostructures by electrochemical deposition technique. The effects of Al doping on the electrochemical, morphologies, microstructures, and optical properties of ZnO nanostructures were studied in detail. The growth mechanism of Al-doped ZnO nanostructures is presumed.

## 2. Experimental Details

### 2.1. Electrochemical synthesis

The deposition solution, prepared with distilled water, contained 0.1 M  $\text{Zn}(\text{NO}_3)_2$ , 1 M  $\text{KNO}_3$  and between 0.05 and 5mM  $\text{Al}(\text{NO}_3)_3$ . The deposition parameters of the AZO films were kept the same as

those for the undoped ZnO film. Deposition temperature was 70° C and pH was in the range of 4 to 6. The deposition process was carried out in a three-electrode cell. The counter-electrode was a platinum wire and the reference electrode was a saturated calomel electrode (SCE, +0.241 V vs. SHE). F-doped SnO<sub>2</sub> (FTO, 20-23 Ωsq.<sup>-1</sup>)-coated transparent glasses were used as a working electrode. The substrates were cleaned ultrasonically in water, acetone and ethanol. They were activated in 45 % HNO<sub>3</sub> for 2 min and finally rinsed with distilled water prior the electrodeposition [5]. The applied potential was -1.7 V vs. SCE. The ZnO nanostructure was deposited in a potentiostatic mode, using a computer-controlled potentiostat/galvanostat (Voltalab 40) as a potential source.

Cyclic voltammetry (CV) was found to offer some note worthy information in the electrodeposition synthesis of zinc oxide thin film. Table 1 shows the bath composition and the electrodeposition conditions employed in the preparation of the thin films.

**Table 1:** Deposition conditions of samples AZO0-AZO3.

Sample	[Al <sup>3+</sup> ] (mM)	pH	E <sub>s</sub> (V/ECS)	N <sub>b</sub> (cm <sup>2</sup> )
AZO0	0	6.5	-0.42	3.11×10 <sup>20</sup>
AZO1	0.05	5.6	-0.37	3.91×10 <sup>20</sup>
AZO2	0.5	4.6	-0.64	4.27×10 <sup>20</sup>
AZO3	5	3.9	-0.95	5.56×10 <sup>20</sup>

## 2.2. Sample characterization

The Mott-Schottky (M-S) analysis for AZO thin films was carried out by conducting a standard electrochemical measurement at 0.2 kHz frequency in a 1 M KNO<sub>3</sub> solution by scanning the potential from positive to negative direction in 50 mV/s steps. The applied potentials were set in the range of -1.0 to + 0.2 V vs. SCE. The crystallographic structure of the thin films was analyzed by a Rigaku Smartlab diffractometer using Cu Kα<sub>1</sub> radiation at 40 kV (Cu Kα<sub>1</sub>, λ = 0.15406 nm). The surface morphology was observed by atomic force microscopy (AFM). The RMS roughness (root-mean-square height deviation) of the samples was obtained directly from the software of the AFM (PicoScan 5.3 from Molecular Imaging). The optical transmittance spectra were obtained with a SHIMADZU 2401PC spectrophotometer in the UV-visible region. The spectra were corrected for glass substrates. All measurements were conducted at room temperature

## 1. Results

### 1.1. Electrochemical characterization

The electrodeposition process of ZnO is well-known; first, the reduction of nitrate ions produces nitrite and hydroxide ions at the cathode. This was followed by the interaction of Zn with hydroxide ions forming zinc hydroxide. After dehydration of these hydroxides, ZnO is formed as a final product. This mechanism of electrodeposition is simply described as follows [6],

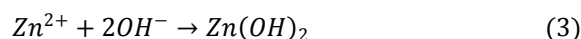
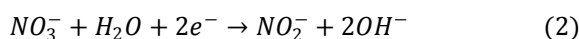
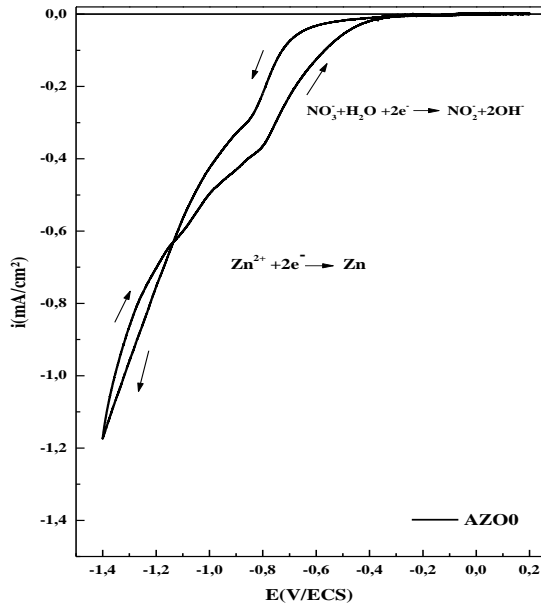
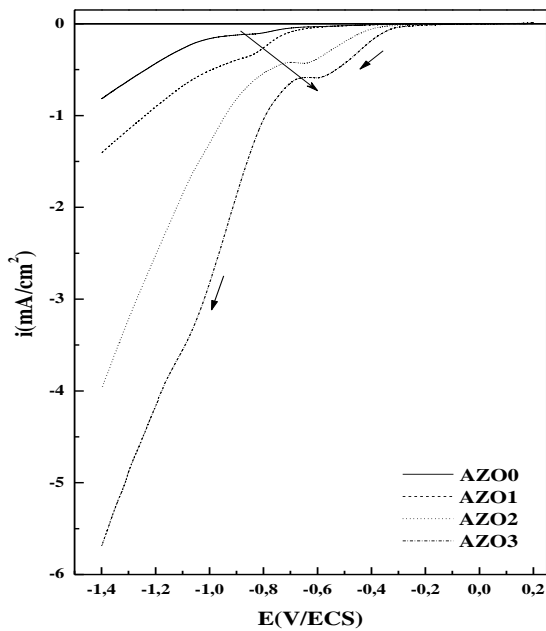


Fig.1 as shown the CV recorded at 70° C in the potential range from +0.2 to -1.4 V vs. SCE in a nitrate solution at 20 mV s<sup>-1</sup>. An increase of the cathodic current density begins around -0.7 V corresponds to the nitrate reduction (reaction 2) [7]. The next increase around -1.1 V corresponds to the reduction of Zn<sup>2+</sup> into metallic Zn. During the reverse anodic scan; no anodic currents were observed denoting thus the good stability of the films which present no reoxidation process.

In order to understand the influence of Al<sup>3+</sup> during the reduction process, voltammetry was also performed at a constant Zn<sup>2+</sup> concentration, and from 0.05 to 5 mM Al(NO<sub>3</sub>)<sub>3</sub> (Fig. 2). For comparison, the curve previously obtained from zinc nitrate solution is also represented on Fig. 2 (curve AZO0). Only the cathodic forward sweeps are shown for the sake of clarity.



**Fig. 1** Cyclic Voltammetry curve recorded for FTO electrode at 70°C in 0.1 M  $\text{Zn}(\text{NO}_3)_2$  and 1 M  $\text{KNO}_3$  solution. The potential scanning rate was 20 mV/s.



**Fig. 2** Cyclic voltammetry curves of the electrolytes used for undoped and Al-doped ZnO growth with different  $\text{Al}^{3+}$  concentration according to Table 1. The scans were performed at a rate of 20 mV/s on FTO substrates.

All cyclic voltammetry curves show a similar feature. With the presence of  $\text{Al}^{3+}$  ions in the solution,  $\text{OH}^-$  ions also react with  $\text{Al}^{3+}$  ions to form  $\text{Al}_2\text{O}_3$ , which incorporates Al into ZnO and thus dopes the ZnO film [1]:



It's clear from Fig. 2, the increase in current density from -0.11 to -0.58  $\text{mA}/\text{cm}^2$  was observed with

increasing of  $\text{Al}^{3+}$  concentration from 0 mM to 5 mM in the electrolyte. The fast increase in current density during electrochemical deposition with Al can be interpreted that  $\text{Al}^{3+}$  accelerated the reduction of  $\text{NO}_3^-$ . This implies catalytic role of  $\text{Al}^{3+}$  to the reduction of nitrate [8].

The semiconductor properties such as donor density ( $N_D$ ) can be measured from the capacitance measurements [9, 10]. In order to determine the effect of the Al concentration on the defects and donor density of the ZnO nanostructures, M-S analysis was performed. The flat band potential ( $E_{fb}$ ) and the charge carrier density for the semiconductor material (ZnO) can be determined using [11]:

$$\frac{1}{C_{sc}^2} = \frac{2}{q\epsilon\epsilon_0 N_D A^2} \left( E - E_{fb} - \frac{kT}{q} \right) \quad (7)$$

where  $C$  is the interfacial capacitance,  $q$  the electron charge ( $1.6 \times 10^{-19} \text{C}$ ),  $\epsilon$  the ZnO dielectric constant ( $\epsilon = 8.5$ ),  $\epsilon_0$  the free space permittivity ( $8.85 \times 10^{-14} \text{F}/\text{cm}$ ),  $A$  the exposed electrode area ( $\approx 1 \text{cm}^2$ ),  $E$  the applied potential across the ZnO space-charge region,  $E_{fb}$  the flat band potential and  $kT/q$  is the temperature ( $T$ ) dependent correction term involving the Boltzmann constant  $k$ . Flat-band potentials and donor densities were calculated from the intercept and slope of the M-S plots respectively. Fig. 3 shows the M-S plot for all the samples of undoped and Al-doped ZnO (AZO). The positive slope of the M-S plot confirms the n type conductivity of the samples. The carrier concentration of AZO thin films increases from  $3.11 \times 10^{20}$  to  $5.56 \times 10^{20} \text{cm}^{-3}$  with the concentration of Al. This range is in agreement with reported carrier concentrations for AZO [12]. It was observed that by increasing the doping concentration, the flat-band potential also changes from -0.42 to -0.95 V vs. SCE.

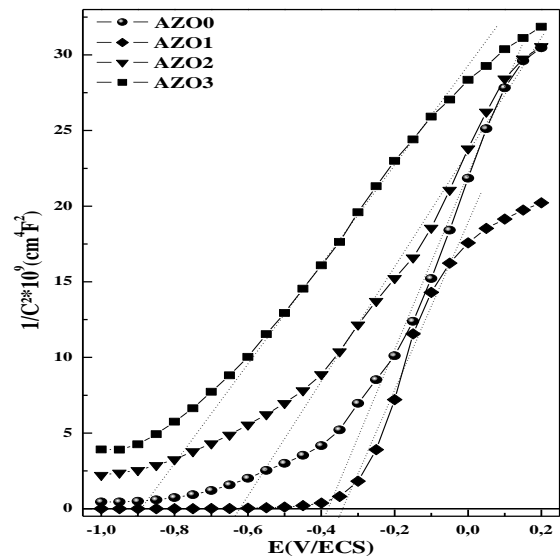


**Fig. 3** Mott-Schottky plots of undoped and Al-doped ZnO (AZO) thin films in 1M  $\text{KNO}_3$  as the electrolyte. Frequency employed was 0.2 kHz.

### 1.2. Morphological analysis

The two-dimensional AFM images of the surface morphologies of ZnO and AZO thin films are shown in Fig. 4. It was found that the films grow with microcrystalline structure. From the images it is seen that all the film surfaces are well covered with the variably distributed spherical grains of varying sizes. It is evidently seen that addition of Al changes the morphology of thin films from clusters into well defined spherical grains. Surface roughness is one of the important properties of the AZO thin films for many opto-electronics applications, because the smooth structure can reduce the scattering of incident light, which makes the contribution to increase the transmittance [13]. Effectively, the surface roughness of the deposited layers is determined by AFM. It is found that the surface roughness is strongly dependent on the concentration of Al in the solution. From this figure, when Al concentration increased from 0.05 to 5 mM, the RMS roughness increased from 5 to 34 nm.

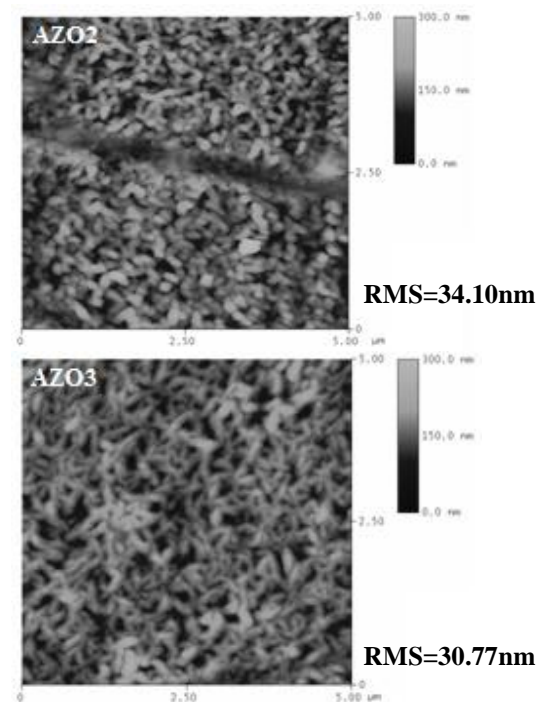
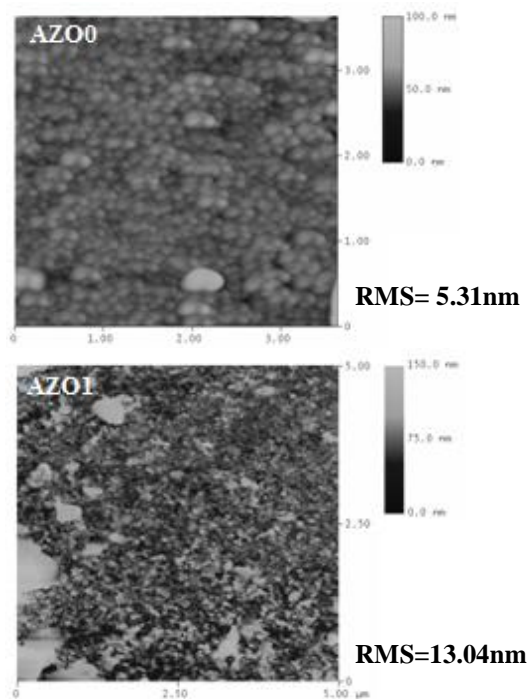


**Fig. 4** AFM images of electrodeposited Al-doped ZnO thin films with different Al content.

It should be noted that the maximum value of RMS was observed at  $C_{Al} = 0.5$  mM and attributed to the rough surface of the AZO film. After this maximum of RMS, the latter decreased as the aluminum concentrations increased.

### 1.3. Structural analysis

The XRD patterns of electrodeposited AZO thin films at different Al concentrations are shown in Fig. 5. These patterns are found to have preferred orientation along (002) plane of the wurtzite structure of ZnO with c-axis normal to the substrate surface. Moreover, the peak intensities of those films decreased with increased Al concentrations. This indicates that an increase in doping concentration deteriorates the crystallinity of films, which may be due to the formation of stresses by the difference in ion size between Zn and Al. On the other hand, the peak position of the (002) plane is shifted to the higher value with the increase of Al doping concentration as shown in the table 2.

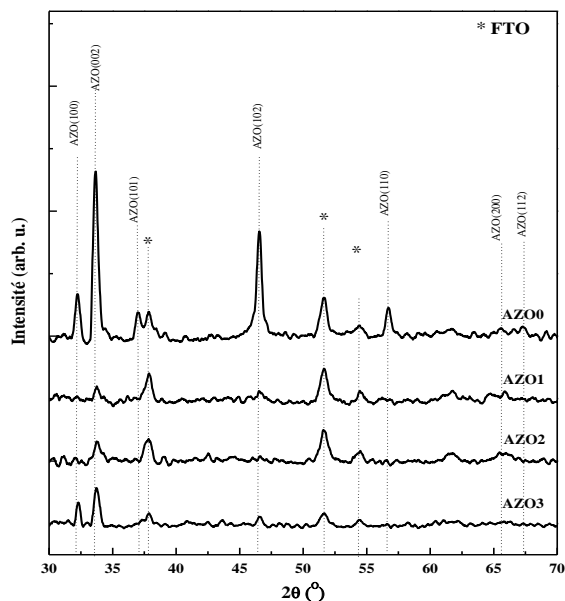


**Fig. 5** Typical XRD patterns of the undoped and Al-doped ZnO nanostructures deposited on FTO substrate at different concentrations of Al.

The shift towards the higher angles may be due to the contraction caused by the substitution of  $\text{Al}^{3+}$  (radius 0.53 Å) on the  $\text{Zn}^{2+}$  sites (0.60 Å) [14]. The average crystallites size can be estimated from the full width at half maximum (FWHM) values of the diffraction peaks. An average size of the crystallites in the direction perpendicular to the plane of the films could be obtained using the Scherrer equation [15]:

$$D = \frac{k\lambda}{\beta \cos\theta} \quad (8)$$

where  $D$  is the crystallite size,  $k$  is a shape factor and usually takes a value of 0.94,  $\lambda$  is the X-ray wavelength ( $\lambda = 1.5406$  Å),  $\beta$  is the FWHM and  $\theta$  is Bragg angle of the given (002) peak. The calculated values of the lattice parameters and average crystallite sizes for ZnO and AZO were summarised in Table 2. When Al doping concentration was increased, the crystallite size of AZO decreased from 36 to 26 nm. Also, the lattice parameters decreases with the increasing the Al content. The reduction of  $a$  and  $c$  parameters may be due to smaller ionic radius of  $\text{Al}^{3+}$  than  $\text{Zn}^{2+}$ .

**Table 2:** The effect of the Al doping concentration on the microstructural and optical properties.

Sample	$2\theta$ (°)	$c$ (Å)	$a$ (Å)	$D$ (nm)	$E_g$ (eV)
AZO0	33.66	5.320	3.258	36.08	3.22
AZO1	33.73	5.310	3.251	28.70	3.41
AZO2	33.73	5.310	3.254	26.65	3.44
AZO3	33.75	5.307	3.249	31.47	3.47

#### 1.4. Optical characterization

Fig. 6a show the optical transmittance spectra of ZnO and AZO thin films deposited on FTO substrates. The value of transmittance increases from 80 % to 90 % with an increase of the Al concentration from 0 to 5 mM. Optical transmission in the visible range is important for TCO applications such as solar cell windows. From the optical absorption spectra, the optical band gap ( $E_g$ ) was calculated by using the well-known Tauc relationship [16]:

$$\alpha h\nu = A(h\nu - E_g)^n \quad (9)$$

Where  $A$  is a constant,  $E_g$  is the band gap of the material, and  $n$  depends on the nature of the transition, being  $n = 1/2$  for direct transitions [17]. It can be seen that the band gap increases from 3.27 to 3.47 eV with the increasing of the Al content [18].

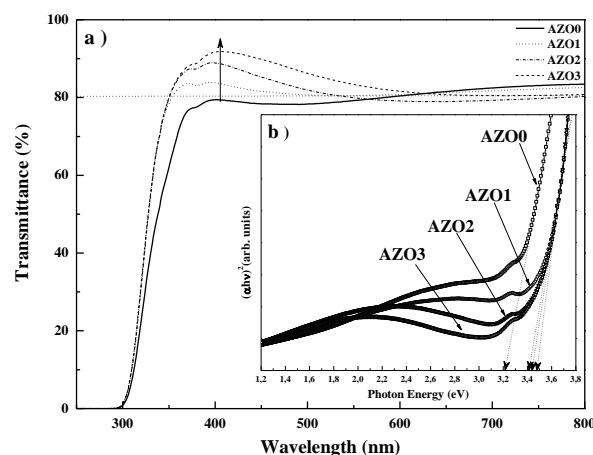


**Fig. 6** Transmission spectra of the ZnO and Al doped ZnO (AZO) thin films electrodeposited on FTO.

The optical absorption edge has a blue shift to the region of higher photon energy with an increase in Al concentration. The blue shift behavior in the band gap can be attributed to an increase in the carrier concentration that blocks the lowest states in the conduction band, known as the Burstein–Moss effect [19]; an increase in the carrier concentration in Al doped ZnO will cause the Fermi level to move into the conduction band. Therefore, the low energy transitions are blocked [20, 21]. The filling of the conduction band by electrons generally causes a blue shift in the band gap.

## 2. Conclusion

Aluminum doped ZnO nanostructures were synthesized by electrochemical method at various Al concentrations. The effects of Al doping on the electrochemical, morphological, microstructural, and

optical properties of ZnO were examined. By addition of Al in the solution, the voltammogram of ZnO shifts the electrodeposition potential in the positive region. Also, the carrier density of the AZO thin film increased from  $3.10 \times 10^{20}$  to  $5.60 \times 10^{20}$   $\text{cm}^{-3}$  with increasing Al concentration. The XRD analysis showed that the crystallinity of the AZO thin films deteriorated as compared to that of ZnO film. The average optical transmittances of AZO films in the visible wavelength range were over 80 %. The high transmittance of > 80 % in Al-doped ZnO allow it to be used as a TCO in solar cells. The optical band gap of the ZnO films shifted from 3.22 eV to more than 3.47 eV after doping.

## References

- [1] X. Han, K. Han, and M. Tao, ECS Transactions, 25 (2010) 93-102.
- [2] O. Lupan, V.M. Guerin, I.M. Tiginyanu, V.V. Ursaki, L. Chow, H. Heinrich, T. Pauporte, J. Photochem. Photobiol, A: Chem, 211 (2010) 65-73.
- [3] M. R. Khelladi, L. Mentar, A. Beniaiche, L. Makhloufi, A. Azizi, J. Mater. Sci., Mater. Electron. 24 (2013) 153-9.
- [4] S. Laidoudi, A.Y. Bioud, A. Azizi, G. Schmerber, J. Bartringer, S. Barre, A. Dinia, Semicond. Sci. Technol. 28 (2013) 115005.
- [5] S. Haller, J. Rousset, G. Renou, and D. Lincot, EPJ Photovoltaics, 2 (2011) 20401
- [6] Izaki M, Omi T 1996 J. Electrochem. Soc. 143 L53
- [7] M.R. Khelladi, L. Mentar, M. Boubatra, A. Azizi, Mater Lett, 67 (2012) 331-333.
- [8] J.A. Cox, A. Brajter, Electrochim. Acta 24 (1979) 517.
- [9] A. Wolcott, W. A. Smith, T. R. Kuykendall, Y. Zhao, and J. Z. Zhang, Adv. Funct. Mater. 19 (2009) 1849 .
- [10] V. K. Mahajan, M. Misra, K. S. Raja, and S. K. Mohapatra, J. Phys. D: Appl. Phys. 41 (2008) 125307.
- [11] J. Rousset, E. Saucedo, D. Lincot. Chem Mater, 40 (2009) 21534
- [12] A. C. Aragonès, A. Palacios-Adrós, F. Caballero-Briones, F. Sanz, Electrochim Acta 109 (2013) 117- 124.
- [13] I. G. Dimitrov, A. O. Dikovska, P. A. Atanasov, T. R. Stoyanchoy, T. Vasilev, J. Phys. Conf. Ser. 113 (2008) 012044.
- [14] S.C. Navale, V. Ravi, S. Mulla, S. W. Gosavi, S. K. Kulkarni, Sensors and Actuators B126 (2007) 382.
- [15] R. Jenkins, R. L. Snyder, Introduction to X-ray Powder Diffractometry, p. 89, John Wiley & Sons, New York (1996).
- [16] J. Tauc. Optical Properties of Solids 22, F. Abeles, Ed., North Holland Pub, Amsterdam, (1970).
- [17] B. Pejova, I. Grozdanov, J. Solid State Chem, 158 (2001) 49.
- [18] O. Baka, A. Azizi, S. Velumani, G. Schmerber, A. Dinia, J Mater Sci: Mater Electron, 25 (2014) 1761-1769.
- [19] E. Burstein, Physical Review, 93 (1954) 632.
- [20] T.S. Moss, Phys. Soc. Lond. B 67 (1954) 775.
- [21] K. Sakai, T. Kakeno, T. Ikari, S. Shirakata, T. Sakemi, K. Awai, T. Yamamoto, Journal of Applied Physics, 99 (2006) 043508.